Magnetic-Induced Luminescence from Flexible Composite Laminates by Coupling Magnetic Field to Piezophotonic Effect

*Man-Chung Wong, Li Chen, Ming-Kiu Tsang, Yang Zhang, and Jianhua Hao**

Luminescent materials, also called phosphors, have been extensively investigated because of their interesting physics and widespread applications.[1,2] The past several decades have witnessed rapid growth in research and development of phosphors, which has stimulated the fields of physics, chemistry, materials science, and optoelectronics. In principle, the types of luminescence may be distinguished by the method of excitation sources. The prefixes to terms of various types of luminescence are usually self-explanatory. For instance, photoluminescence (PL) is excited by photon energy while electroluminescence (EL) is stimulated by electric field, and so on. The most frequently used PL and EL materials are central to a wide variety of devices and systems, including display, light-emitting diode (LED), sustainable energy devices, and biomedicine.[3–6] Compared to the stimulation by photon and electric field, little work is reported on the light emission by another common source, i.e., magnetic field. The correlation between light emission and magnetic field stimulation has often been ignored in our common knowledge of luminescence. In most reports,[7–9] the term of magnetoluminescence (ML) with a prefix of "magneto" is about PL or EL under the influence of externally applied magnetic field, which does not mean the magnetic-induced luminescence (MIL). ML has previously been observed in some luminescence systems, such as semiconductor nanostructures and organic compounds based on intercharge spin–spin interaction, spin-dependent excited processes, and Lorentz effects.[8] Notably, the ML effects typically occur under extreme conditions of high magnetic field and low temperature. By comparison, the realization of light-emission stimulated by magnetic field faces an even greater challenge and hence the phenomenon of intrinsic MIL is extremely rare. The long-standing problem limits our understanding of the relationship between magnetic field and luminescence, hindering potential applications of both magnetic and luminescent materials. It is worthy of attention that the availability of various types of laminate structures with great flexibility of design makes it possible to tailor their properties via interfacial coupling. By considering that the direct magnetic–luminescence coupling is exceptionally difficult to realize in a single phase, the development of composite laminates may be an alternative solution to tackle the major problem at this stage, particularly the practical approach based on composite laminates should be favorable for many magnetic applications. In real world, magnetic fields exist in many systems, and therefore the detection of magnetic field is essential for environmental surveillance, mineral exploring, and safety monitoring. For example, the large magnetic flux generated from a grid-connected power wire can be used to monitor power consumption of electric appliances in power industry.[10] It is known that conventional magnetic sensing materials and devices are restricted to employing the conversion from magnetic field input to electric signal output, such as Hall, magnetoresistive, and magnetoelectric effects, as well as recently developed nanogenerator mode.[11–13] The sensor nodes are usually mounted on the power wire of each appliance. It is essential to explore more approach beyond the magnetoelectric process. Therefore, it would be very attractive if MIL-based laminate materials and devices are conceived, which are capable of showing the ability of responding and harvesting energy from magnetic fields. In contrast to conventional magnetic sensors, the MIL-based devices enjoy competitive advantages, including real-time visualization, remote sensing without making electric contact, nondestructive and noninvasive detection.

It is noticeable that Wang proposed piezophotonic effect, [14] which can be regarded as a two-way coupling effect between piezoelectricity and photoexcitation properties as shown in **Figure 1**a. In this research field, the strain-induced piezoelectric potential can be utilized for improving the performance of optoelectronic and energy devices based on the piezophotonic and piezophototronic effects.[15–20] In our previous works,[21,22] we have taken advantage of piezoelectric $Pb(Mg_{1/3}Nb_{2/3})O_3$–$PbTiO_3$ substrate-induced strain coupling and observed light and ultrasound emissions from hybrid thin-film structures. However, the coupling between magnetic field and piezophotonic effect which may lead to MIL as shown in Figure 1a has not yet been exploited. In this work, we have proposed a practical approach to design and fabricate composite laminate systems composed of magnetic actuator and phosphor materials. Novel MIL phenomenon has first been observed from the flexible composite laminates via strain-mediated coupling, resulting in the green and white light emissions by the naked eyes. Interestingly, the achieved light emissions of the material systems can be modulated in reversible and dynamical manners under the control of low magnetic field occurring at room temperature. We have demonstrated low magnetic field driven green light emission pattern and white light source based on the new MIL materials, which may offer the potential to develop some new concept devices, such as remote magnetic-optical sensor, memory devices, energy harvester, and so on.

M.-C. Wong, L. Chen, M.-K. Tsang,
Dr. Y. Zhang, Prof. J. Hao
Department of Applied Physics
The Hong Kong Polytechnic University
Kowloon, Hong Kong, P. R. China E-
mail: jh.hao@polyu.edu.hk
M.-C. Wong, L. Chen, M.-K. Tsang,
Dr. Y. Zhang, Prof. J. Hao
The Hong Kong Polytechnic University Shenzhen
Research Institute
Shenzhen 518057, P. R. China

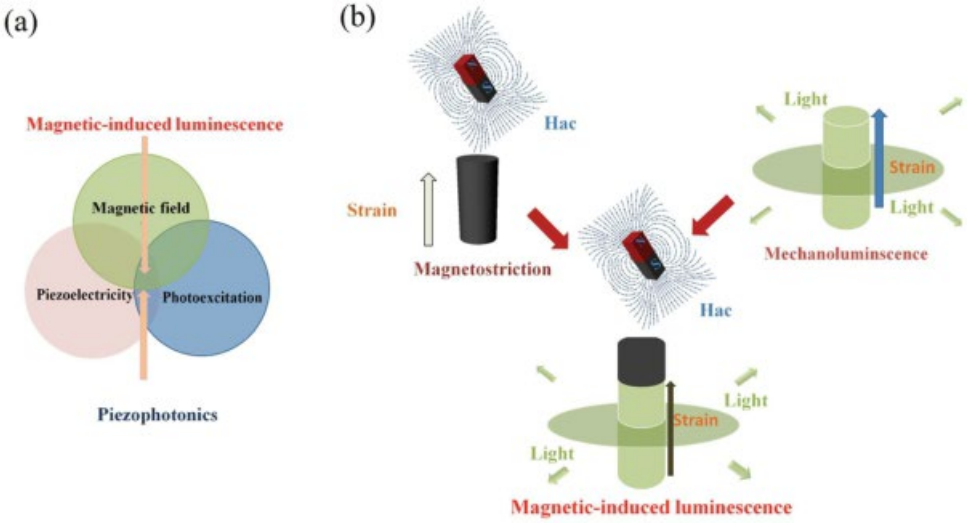

Figure 1. a) Schematic diagram illustrating the field of piezophotonics and MIL. b) Implementation of MIL effect based on strain-mediated magneto-luminescent coupling in two phases of magnetic elastomer and mechanoluminescence phosphor.

Figure 1b depicts a strategy of practical approach to realize MIL in this work, namely strain-mediated magnetoluminescent coupling in two phases where the magnetic and photon parameters arise in separate but intimately connected phases. Such MIL is a result of the product of the magnetostrictive (magnetic/mechanical) effect in the magnetic phase and mechanoluminescence (mechanical/luminescent) effect in the phosphor one, namely,

$$\text{MIL}=\frac{\text{magnetic}}{\text{mechanical}}\cdot\frac{\text{mechanical}}{\text{luminescent}} \tag{1}$$

Assume that an external magnetic field (H) is applied to the strain ($\int$) coupled by the two-phase system, thus magnetostrictive coefficient $\lfloor$ in a magnetic-phase can be described by

$$\lfloor=\frac{\partial\int}{\partial H} \tag{2}$$

On the other hand, luminescent intensity (I) of mechanoluminescence is proportional to the strain and its rate of change ($\partial\int/\partial t$), which can be written in the form [23,24]

$$I=\langle\int\frac{\partial\int}{\partial t}(1-\exp(-t/\rceil)) \tag{3}$$

where $\langle$ is a constant of coupling strain to luminescence; $\rceil$ is lifetime of the interaction associated with mechanoluminescence event. Therefore, the MIL intensity in the strain-mediated two phases triggered by magnetic field can be expressed as

$$I=\langle\lfloor\circledR\int\frac{\partial H}{\partial t}(1-\exp(-t/\rceil)) \tag{4}$$

where ® is a coupling factor between the magnetic and phosphor phases (®δ 1). For some magnetic actuators maintaining the linear relationship of $\int$ and H with correlation coefficient c under certain operation range, Equation (4) can be further described as

$$I=\langle\lfloor\circledR cH\frac{\partial H}{\partial t}(1-\exp(-t/\rceil)) \tag{5}$$

For $t >> \rceil$, Equation (3) can be simplified as

$$I=\langle\int\frac{\partial\int}{\partial t} \tag{6}$$

By integrating Equation (6) when taking $\int = 0$ at $t = 0$, we obtain

$$\int_0^t I\,dt=\int_0^{\int_0}\langle\int d\int \tag{7}$$

where $\int_0$ is the maximum value of the applied strain. From Equation (7), the total luminescence intensity I_T is

$$I_T=\frac{1}{2}\langle\int_0^2 \tag{8}$$

When substituting the integral result of Equation (2) into Equation (8) and taking into account coupling factor between the two phases, we find

$$I_T=\frac{1}{2}\langle\lfloor\circledR H_0^2 \tag{9}$$

where H_0 is the maximum value of the magnetic field.

Hence, the total luminescence intensity of MIL is proportional to the product of the three parameters ($\langle$, $\lfloor$, ®) and square of H_0. According to Equation (4), it is apparent that static dc magnetic field is unable to excite the luminescence because of $\partial H/\partial t = 0$. For alternating ac magnetic field, e.g., $H = H_0\sin\rceil t = \sqrt{2}H_{rms}\sin\rceil t$, where H_{rms} is the

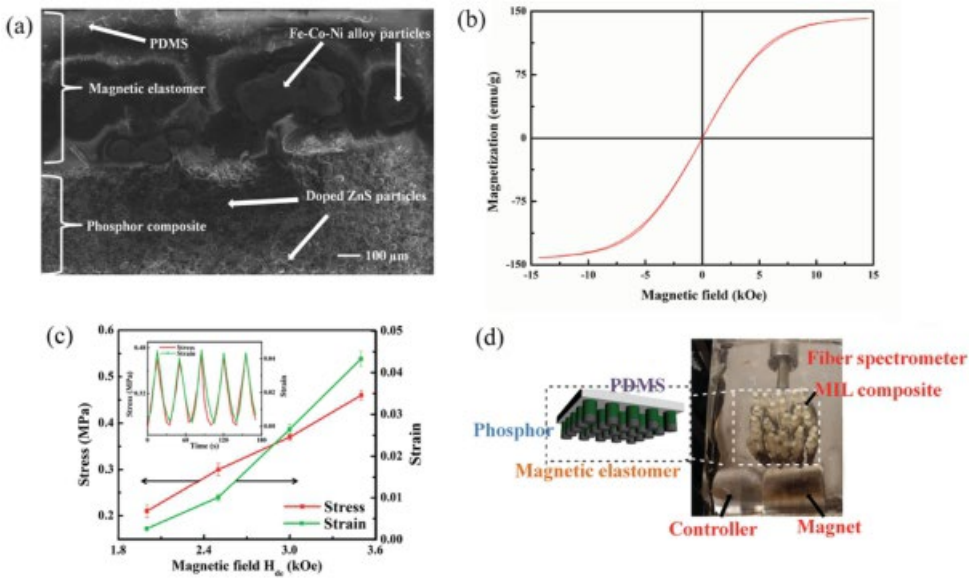

Figure 2. a) SEM image taken at the interface of the synthesized PDMS polymer composite laminate consisted of Fe–Co–Ni alloy particle-based magnetic elastomer and metal-ion-doped ZnS microparticle-based mechanoluminescence phosphor. b) Room temperature magnetization of the magnetic elastomer versus magnetic field measured by VSM. c) Stress exerted onto the magnetic elastomer and strain induced versus applied dc magnetic field strength. Inset shows the cycling test, in which the imposed cyclic period time was 30 s when switching from 2 to 3.5 kOe of field strength. d) The setup used for MIL measurements and device demonstration.

root-mean-square magnetic field, MIL intensity will depend on the amplitude and frequency of the input magnetic field.

To verify the hypothesis, we have synthesized multiphase rods consisted of the composite of metal-ion-doped ZnS microparticles mixed to polydimethylsiloxane (PDMS) and another composite of magnetic Fe–Co–Ni alloy particles mixed to PDMS. The microstructure of the resultant composite is shown in the scanning electron microscopy (SEM) image of **Figure 2**a. ZnS is chosen as phosphor host here because of its excellent piezoelectricity. Previous studies have proved that the piezoelectric potential is capable of triggering the luminescent center of metal-ion dopants, resulting in the light emissions when the flexible composites of metal-ion-doped ZnS microparticles embedded in PDMS are stimulated by external strain.[22,25,26] On the other hand, the designed magnetic composite consisted of PDMS mixed with magnetic particles can response to external magnetic field and then exhibit large deformation,[27,28] which can serve as magnetic actuator to stimulate the doped ZnS in the hybrid system as shown in Figure 1b. PDMS composite is very useful due to its features of softness, optical transparence, ease of fabrication, mechanical robustness, and low cost.[26] In this experiment, PDMS serves as a packaging material and also delivers the generated strain from magnetic part to the phosphor part under magnetic field. In order to observe magnetic responsive luminescence, the design of the three components of polymer, magnetic particle, and phosphor should be optimized to reach a compromise between elastic module, magnetic permeability, luminescence, and other requirements in the hybrid structure.[29] Therefore, the magnetic and elastic properties of the magnetic responsive polymer are first measured in our experiments by applying magnetic field along the axial direction of the cylindrical samples.

Figure 2b presents the magnetization of Fe–Co–Ni alloy + PDMS composite as a function of applied magnetic field at room temperature measured from vibrating sample magnetometer (VSM). The chosen Fe–Co–Ni alloys are conventional soft magnetic materials widely used in industry since they have a very low coercive field and high saturation magnetization. As shown in Figure 2b, the magnetic behavior of the composite can be approximately considered as linear behavior with no significant hysteresis because of negligible coercive field (H_c H 9 Oe), when applying magnetic field within the range of several kOe where our operating magnetic fields are located in the subsequent measurements. This is a desirable feature in generating strain leading to MIL in our application since the complications arising from remanent magnetization could be avoided. Figure 2c shows the elastic properties of Fe–Co–Ni alloy + PDMS composite under varied magnetic field stretching along the axis of cylindrical sample. It indicates that both strain and stress increase monotonically when the dc magnetic field increases from 2 to 3.5 kOe, implying that the designed PDMS mixed with Fe–Co–Ni alloy can serve as a magnetic elastomer for sensing and actuation application.[30] The inset of Figure 2c presents the experienced stress and strain versus time while cycling the external magnetic field. The imposed cyclic period time was 30 s when switching from 2 to 3.5 kOe of field strength. Our experimental test shows that the strain and stress of the magnetoactive elastomer from cycle to cycle are almost maintained and reproducible after many cycles of operation (five cycles as an example are presented in the inset of Figure 2c), making it durable and reliable for MIL application described in a later section. For the design of the magnetoactive elastomers, the magnetoelastic ratio (MER) can be used to quantify the propensity of a rod-like sample under magnetic field, which is defined as MER = $\lceil_0 M_2\rangle_2/E$, where μ_0

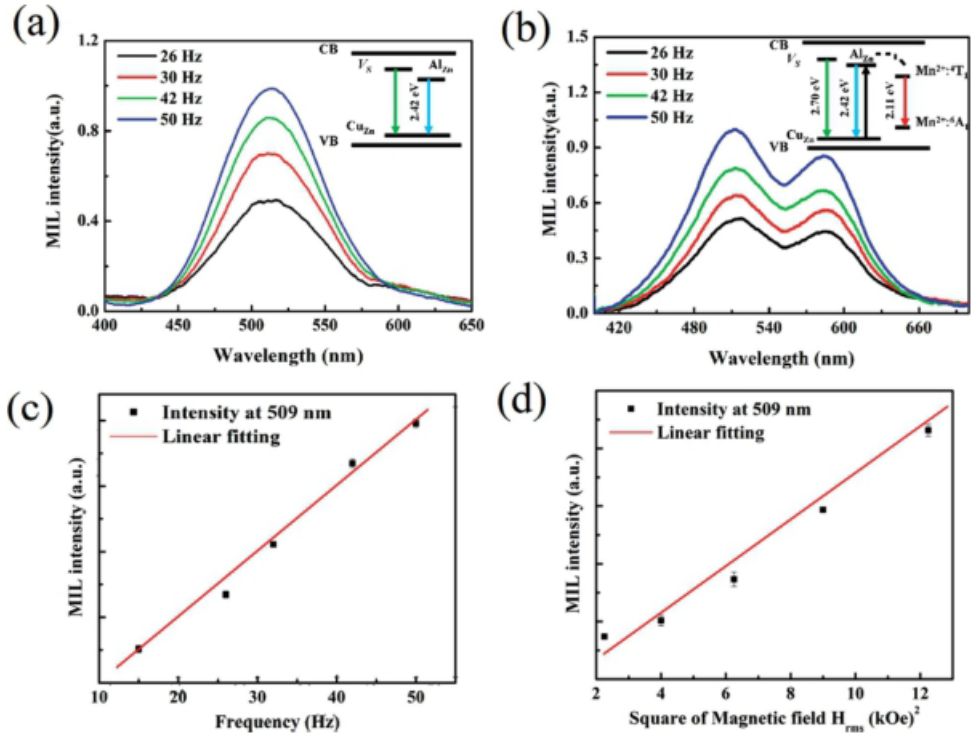

Figure 3. a) Luminescence spectra of Al, Cu-doped ZnS phosphor combined with Fe–Co–Ni + PDMS composite laminate activated by ac magnetic field with the frequency between 26 and 50 Hz. The inset shows the energy level diagram. b) Luminescence spectra of Al, Cu, Mn-doped ZnS phosphors combined with Fe–Co–Ni + PDMS composite laminate activated by alternating magnetic field with the frequency between 26 and 50 Hz operated at room temperature. The inset shows the energy level diagram. c) MIL intensity at 509 nm measured from Al, Cu-doped ZnS-based composite as a function of frequency under ac magnetic field of H_{rms} = 3.5 kOe operated at room temperature. The inset shows the energy level diagram. d) MIL intensity at 509 nm measured from Al, Cu-doped ZnS-based composite as a function of the square of H_{rms} under the frequency of f = 50 Hz.

is the magnetic permeability of vacuum, M is the magnetization, ⟩is the mass density, and E is the Young's modulus of the composite.[29] In our case, the Young's modulus for the sample is calculated to be 70 MPa under a zero magnetic field. Therefore, large M and small E obtained from our fabricated polymer composites would be benefit to the desired magnetoelastic response. In order to produce efficient magnetic response, this kind of the magnetoactive elastomer with composite structure should exhibit a compromise between flexibility and magnetic permeability. The amount of deformation generated depends on the size and concentration of the magnetic particles incorporated into polymer matrix. In principle, large sized magnetic particles yield a strong magnetization, while weak magnetization is generated from small sized particles. For example, the incorporation of more amounts of Fe–Ni–Co alloy particles into the elastomeric polymer matrix will generally achieve higher magnetic permeability and hence give rise to larger deformation and strain under given magnetic field. However, adding high-ratio Fe–Co–Ni alloy particles to a composite increases the modulus of the composite as well. Furthermore, the composite with high concentration of magnetic particles becomes more compact and therefore there has no enough space to shrink or swell within confined space of the polymer scaffolding. Such inappropriate design will result in a less flexible material with reduced strain delivered to phosphor phase. Therefore, it is important to optimize the loading of magnetic particles in order to produce most magnetic responsive material in this study.

With the magnetic elastomer, we prepared MIL rods that consist of metal-ion-doped ZnS + PDMS (upper side) and Fe–Co–Ni alloy + PDMS (bottom side). As shown in Figure 2d, these MIL rods can be assembled on a plate or encapsulated into a mould made from transparent polymers (e.g., PDMS) to fabricate a luminescent matrix for further measurements and device demonstration. As aforementioned, a number of studies have indicated that the strain-induced luminescence from metal-ion-doped ZnS is essentially a dynamical process.[21–26] According to our proposed MIL model as above, time-varying magnetic fields were therefore provided by rotating an NdFeB permanent magnet with a controller in the setup of MIL test (Figure 2d). The strength and frequency of magnetic field can be readily modulated through adjusting the magnet–sample distance and rotation speed of a controller. When the alternating magnetic field acts on the sample, the transient strain produced in Fe–Co–Ni + PDMS side will deliver to the metal-ion-doped ZnS + PDMS side and subsequently generate light recorded by optical fiber spectrometer.

When applying magnetic fields with the controller's frequency f of 26–50 Hz, the luminescence spectra of Al, Cu-doped ZnS, and Al, Cu, Mn-doped ZnS phosphors combined with Fe–Co–Ni + PDMS are shown in **Figure 3**a,b, respectively. On the whole, the obtained MIL emission profiles are quite similar to the previously observed PL, EL, and mechanoluminescence spectra from the corresponding phosphors.[22,25,26] In Figure 3a, the dominant peak is seen at 509 nm, which can

be explained from the donor–acceptor (D–A) recombination of $Al_{Zn}^{\bullet}$ – Cu_{Zn} as shown in the inset of Figure 3a. As illustrated in Figure 1a, MIL is as a result of coupling between magnetic field and piezophotonic effect. The phosphor phases of metal-ion-doped ZnS used in this work possess a wurtzite-type noncentral symmetric structure and inherently exhibit piezoelectric characteristics. When applying magnetic fields to the composites, the strain generated by the magnetic elastomer gives rise to an inner piezoelectric potential in the metal-ion-doped ZnS particles. A number of previous studies suggest that the piezoelectric potential is capable of varying the band structure of semiconductors under strain application.[14–18] Hence, when magnetic fields trigger strain and give rise to piezoelectric field in the metal-ion-doped ZnS, the carriers in the luminescent center are excited to a higher energy level. Subsequently, luminescence is induced by the electron–hole (e–h) recombination. It is noted that the piezoelectric potential created by the strain in the metal-ion-doped ZnS has a polarity. Since alternating magnetic fields are employed in our measurement, the structure should experience tensile and compressive strains in one cycle, which would induce piezoelectric potential with opposite polarity in the metal-ion-doped ZnS. Such effect may result in the different response of luminescence at the rising and falling edges, which has been studied in our previous reports.[21,22] In Figure 3b measured from Al, Cu, Mn-doped ZnS, there are two main peaks centered at 525 and 588 nm. To understand the origin of the emissions, the inset of Figure 3b depicts the schematic illustration of band diagram of Al, Cu, Mn-doped ZnS. Briefly, the sulfur vacancies (V_S) in ZnS compound may trap electrons to form shallow donor levels, while Al^{3+} ion substitutionally occupies the Zn^{2+} site (Al_{Zn}) to generate another donor levels, and Cu^{+} substituted for Zn^{2+} (Cu_{Zn}) may create acceptor level which can trap holes. From this energy level diagram, one may expect three light-emission peaks, namely the intense light emission at 2.42 eV originates from the D–A pairs recombination between $Al_{Zn}^{\bullet}$ – Cu_{Zn}, while another main band peaked at 2.11 eV is due to the radiation energy transition between $^4T_1$ and $^6A_1$ of Mn^{2+} ion. The Mn^{2+} ion related emission is deduced to an effective nonradiation energy transfer from $Al_{Zn}^{\bullet}$ – Cu_{Zn} to Mn_{Zn}. Apart from the two main peaks, the D–A type emission process of $Al_{Zn}^{\bullet}$ – Cu_{Zn} may cause a minor emission band of luminescence spectrum around 2.70 eV (H460 nm). These three emission bands can result in the overall white light emission. In Figure 3b, the minor shoulder band of luminescence spectrum at 460 nm seems to be very weak. It is likely that the stretching stress and frequency induced by alternating magnetic field during measurement is insufficient to activate the blue emission because of the softness of PDMS.[22,26] According to Figure 3a, the MIL emissions peaks at 509 nm of the composite remain almost unchanged when varying *f*. Similarly, there has been no observable wavelength shift at 509 nm under different strength of magnetic field (not shown). The conditions allow one to investigate the relationship between MIL at the fixed wavelength of 509 nm and the conditions of applied magnetic fields (*f* and H_{rms}). Figure 3c,d shows the MIL intensity peaked at 509 nm from Al, Cu-doped ZnS as a function of *f* and the square of H_{rms}, respectively. It is noticeable that the MIL intensity increases linearly when increasing either *f* or H_{rms2}, which is consistent with the proposed MIL model as above. The observed phenomena also accord with the result as shown in Figure 2c, where the magnitude of strain is enhanced with an increase in the strength of magnetic field. Hence, more charge carriers are detrapped when increasing the magnitude and change rate of magnetic field, resulting in the enhancement of e–h recombination and MIL. Importantly, the linear relationship of MIL intensity versus *f* and H_{rms2} as shown in Figure 3c,d should benefit to developing novel MIL-based magnetic sensors when considering that good linear relationship between the output and input signals is preferred in practical application.[13]

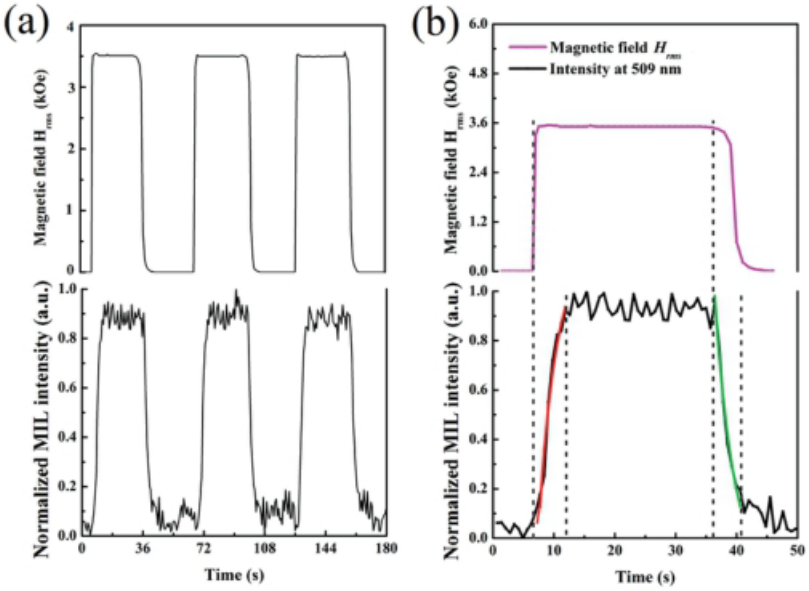

Figure 4. a) Transient characteristic of MIL from the Al, Cu-doped ZnS green-phosphor-based composite. Applied ac magnetic field strength H_{rms} versus time (upper) and MIL intensity peaked at 509 nm versus time (lower). b) Enlarged graphs of single cycle. The rising and falling edges of MIL can be fitted to exponential growth (red) and decay (green) functions.

Figure 4a shows the transient characteristic of MIL from the Al, Cu-doped ZnS green-phosphor-based composite. In this measurement, ac magnetic field with the frequency of 50 Hz was initially switched on and retained at H_{rms} = 3.5 kOe for 30 s and subsequently switched off. In response to the switching cycle of H_{rms} from 0 to 3.5 kOe, MIL intensity peaked at 509 nm rises until its saturated value when the ac magnetic field is switched on and then begins to fall towards zero when the ac magnetic field is decreased from the maximum value of 3.5 kOe to 0 as expected. To shed more light on the interesting tunable MIL, we have enlarged a single cycle as shown in Figure 4b. There is approximately exponential increase and decrease in the MIL intensity under time-varying amplitude of

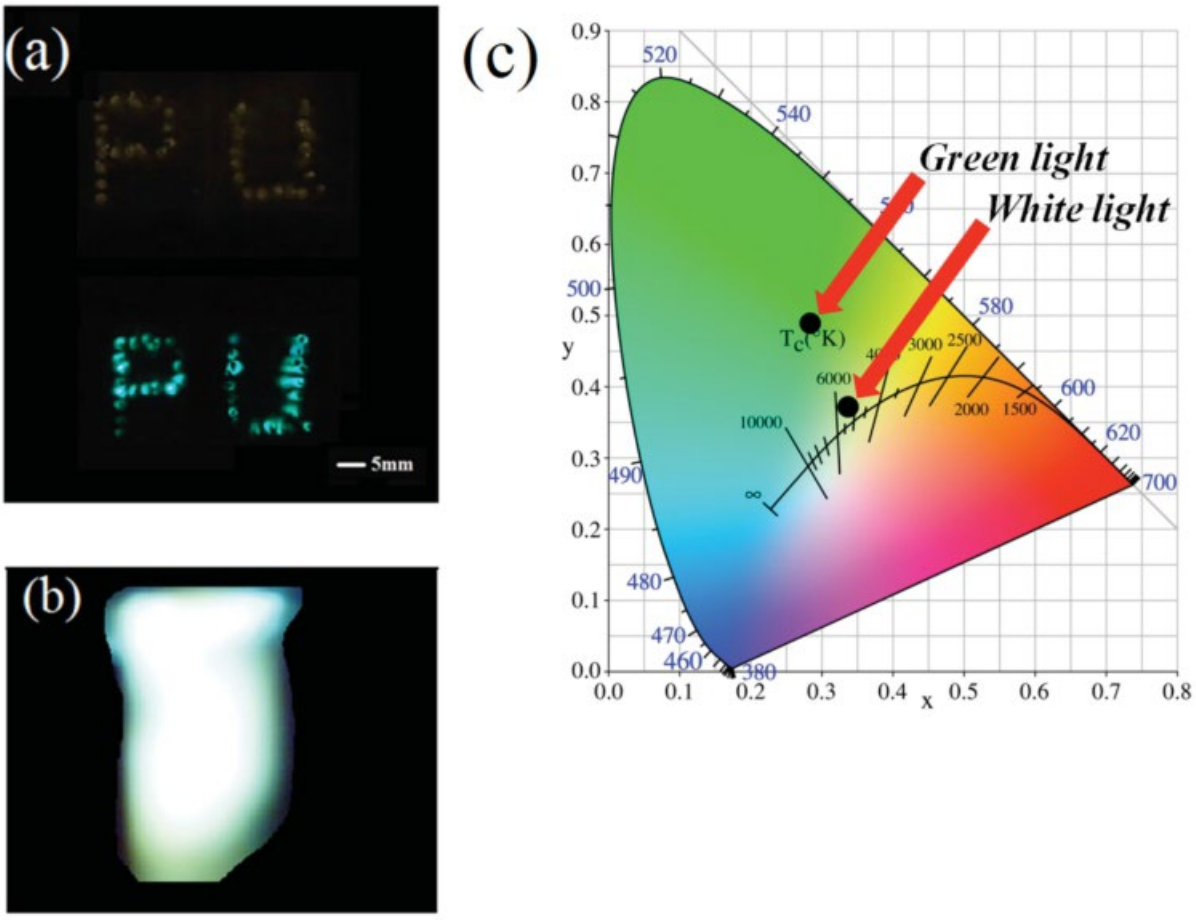

Figure 5. a) Photograph of displaying green colored logo "PU" representing the abbreviation for the Hong Kong Polytechnic University from MIL materials driven by low magnetic field without (upper) and with magnetic field (lower). b) White color emission of MIL light source under magnetic field. Both green letters and bright white source can be seen by the naked eyes. c) CIE diagram showing the green and white lights of the obtained MIL-based pattern and light source, respectively.

ac magnetic field. In other words, the rising and falling edges of MIL responding the changes in H_{rms} can be fitted as exponential growth and decay functions, respectively. According to the fitting curves as shown in Figure 4b, the rise time (r) and the fall time (f) are determined to be 2.85 and 3.15 s, respectively. It should be pointed out the rise time serves as the response time of the MIL phosphor composite in the device applications. Moreover, the figure of merits of the novel type of device will highly depend on the constant of coupling strain to luminescence (), magnetostrictive coefficient (), coupling factor between the magnetic and phosphor phases (®) and so on based on our proposed MIL model. At any rate, the obtained result shown in Figure 4a demonstrates the modulation of the luminescence in reversible and dynamical manners with time-varying magnetic field applied to MIL composites, which should be very promising to design and make new concept of magnetic-luminescence devices.

In order to show the potential of applying MIL phenomena to potential applications such as display and white lighting, we have made patterned arrays as illustrated in **Figure 5**. In the measurements, the magnetic field of H_{rms} = 3.5 kOe with the frequency of 50 Hz was employed at room temperature. With Al, Cu-doped ZnS-based MIL composites, we display green colored logo "PU" representing the abbreviation for the Hong Kong Polytechnic University as shown in the photograph of Figure 5a. In addition, Figure 5b illustrates white-light emission from MIL made by Al, Cu, Mn-doped ZnS-based composites. Both green letters and bright white source can be seen by the naked eyes. Figure 5c presents conventional Commission Internationalede L'Eclairage (CIE) diagram of the observed green and white light emissions. Accordingly, **Table 1** lists the performance parameters of the two kinds of light emissions, including CIE, correlated color temperature (CCT), luminance or brightness, and MIL efficiency. For particular white light emission in the table, the CIE coordinates are found to be (0.3462, 0.3735) and hence the CCT is determined to be 5027 K, indicating the obtained MIL phosphor composite emits a somewhat cool white color. Since this work represents the first example of MIL materials and devices, there has been no existing data of the device's figure of merits for comparison. It is known that power consumption is one of figure of merits in PL and EL devices, such as flat-panel displays and light sources. Typically, the unit lm W□ is used in EL device, where lumen (lm) and watt (W) are units for describing light-emission

Table 1. Performance parameters of the two light emissions based on MIL composite laminates.

Luminescence type	CIE (x, y)	CCT [K]	Luminance [cd m□]	Efficiency [lm Oe□]
Green	(0.2893, 0.4884)	n/a	21	0.0014
White	(0.3427, 0.3735)	5027	19	0.0013

output and electrical input, respectively. By analogy with EL, in this table, we define the MIL efficiency of the new type of device driven by magnetic field as | H light emission output/ magnetic field input strength in the unit of lm Oe□. Up to now, commercial display products are dominated by liquid-crystal display and LED devices, while solid-state lighting technology is based on semiconductor LED and LED pumped phosphor. All of these devices are electrically driven. In our results, the display and light sources are driven by magnetic field, providing a new insight and possibility for display and solid state lighting applications in some specific situation where alternating magnetic fields are applicable. It is remarkable that our developed MIL materials and devices possess flexible, contactless and free of electric power features, which are attractive for future magnetic sensing and energy harvesting applications.

In conclusion, a strategy is proposed to observe an unexplored phenomenon, namely MIL by combining magnetic and piezophotonic effects. The implementations of the new concept are based on the design and fabrication of MIL composite laminates that consist of metal-ion-doped ZnS + PDMS and Fe–Ni–Co alloy + PDMS. Novel MIL phenomenon has been observed from the phosphor composites via strain-mediated coupling. Interestingly, the unusual light emissions of the material systems can be modulated in reversible and dynamical manners under the control of time-varying magnetic field as low as H_{rms} H 3.5 kOe at room temperature. The experimental observations accord with our proposed MIL model. The proof-of-concept MIL devices have been demonstrated, showing the pattern of green colored logo and white color light sources by the naked eyes. Such a new type of device is capable of sensing or converting a dynamic magnetic action without need of using a power unit to the device. The device performance parameters, including CIE, CCT, luminance, and power efficiency have been tested. Our results not only provide a new family member in both phosphor and magnetic materials to observe novel MIL phenomenon but also offer the new possibility to find prospective device applications, such as remote magnetic-optical sensor, memory devices, energy harvester, nondestructive environmental surveillance, and stimuli-responsive multimodal bioimaging.[31]

Experimental Section

Synthesis of MIL Composites: Acrylonitrile butadiene styrene (ABS) mold composed of 25 holes, each with a diameter of 1 mm and a depth of 5 mm was made. Simultaneously, another mold was fabricated by polymethyl methacrylate (PMMA), also consists of 25 elements, each with a diameter of 0.5 mm and a length of 3 mm. Then, ZnS:Al,Cu/ ZnS:Al,Cu,Mn microparticles with the average size of 23 μm were uniformly mixed in PDMS with a weight ratio of 7:3 and poured into the PMMA mould. After curing the composite at 70 °C for 2 h, the rods were extracted and inserted into each hole of the ABS mould which half filled with magnetic responsive polymer. The magnetic responsive polymer consists of magnetic Fe–Co–Ni alloy particles with the average size of 100 μm embedded in uncured PDMS in weight ratio of 2.5:1. Then, the samples were degassed for 30 min to ensure good adhesion between the ZnS:Cu,Al/ZnS:Al,Cu,Mn-doped PDMS rods and the Fe–Co–Ni alloy particle-doped uncured PDMS. After degassing, the mold was put into oven with 110 °C for 24 h to cure the polymer. After removal of the ABS mould, multiphase composites with magnetic actuator phase and mechanoluminescence phosphor phase can be obtained.

Morphology, Magnetic, and Elastic Characterizations: The morphology of the composite was studied using a scanning electron microscope (JEOL JSM-6335F). A Lakeshore 7400 VSM was used to measure the magnetic properties of the magnetic elastomer when scanning magnetic field from □5 to 15 kOe at room temperature. An in-house stress sensor (Wogu digital force gauge Zu-50) was employed for stress characterization. The strain induced from the magnetic elastomer was characterized using a digimatic indicator (Mitutoyo 112 AMB) and an optical gauge.

Luminescence Measurements of MIL: The luminescence spectra were characterized by an Ocean optics spectrometer USB4000 charged-coupled device (CCD) spectrometer (JEOL, Japan) with sampling time of 700 ms. The samples for the spectrum collection experiment were held in a stable platform using a clamp at 0.15 to 5 mm away from a moving NdFeB permanent magnet with static dc magnetic field strength of about 6 kOe. The magnetic strength and frequency of the alternating magnetic field were provided by a rotating NdFeB permanent magnet with various distances from the samples, controlled by an electric motor with variable rotation speed. The magnetic field strength was measured by a Gaussmeter (GM05 Hirst magnetic instruments Ltd.) with dc and ac modes. A spectroradiometer (PR-670 Photo Research Inc.) was used to measure color properties, such as CIE coordinates, luminance, and CCT. The light-emitting images were captured by a digital camera (Olympus PEN Lite E PL3). All measurements were carried out at room temperature.

Acknowledgements

The research was financially supported by the grants from Research Grants Council of Hong Kong (GRF No. PolyU 5005/13P) and National Natural Science Foundation of China (Grant No. 11474241). The PolyU University Research Facility in Materials Characterization and Device Fabrication is acknowledged for providing technical support.

[1] K. Y. Sasaki, J. B. Talbot, *Adv. Mater.* **1999**, *11*, 91.
[2] G. X. Bai, M. K. Tsang, J. H. Hao, *Adv. Opt. Mater.* **2015**, *3*, 431.
[3] H. M. Zhu, C. C. Lin, W. Q. Luo, S. T. Shu, Z. G. Liu, Y. S. Liu, J. T. Kong, E. Ma, Y. G. Cao, R. S. Liu, X. Y. Chen, *Nat. Commun.* **2014**, *5*, 4312.
[4] H. Q. Wang, M. Batentschuk, A. Osvet, L. Pinna, C. J. Brabec, *Adv. Mater.* **2011**, *23*, 2675.
[5] Y. Zhang, J. H. Hao, *J. Mater. Chem. C* **2013**, *1*, 5607.
[6] S. L. Gai, C. X. Li, P. P. Yang, J. Lin, *Chem. Rev.* **2014**, *114*, 2343.
[7] C. V. Dewitz, F. Hatami, M. Millot, J. M. Broto, J. Léotin, W. T. Masselink, *Appl. Phys. Lett.* **2009**, *95*, 151105.
[8] M. Shao, L. Yan, H. P. Pan, I. Ivanov, B. Hu, *Adv. Mater.* **2011**, *23*, 2216.
[9] N. Koche, F. Plentz, W. N. Rodrigues, M. V. B. Moreira, A. G. Oliveira, J. C. Gonzales, *Physica B* **2001**, *298*, 295.

[10] Y. Tang, F. Blaabjerg, P. C. Loh, C. Jin, P. Wang, *IEEE T. Power Electr.* **2015**, *30*, 1855.
[11] M. Johnson, B. R. Bennett, M. J. Yang, M. M. Miller, B. V. Shanabrook, *Appl. Phys. Lett.* **1997**, *71*, 974.
[12] J. Ma, J. M. Hu, Z. Li, C. W. Nan, *Adv. Mater.* **2011**, *23*, 1062.
[13] Y. Yang, L. Lin, Y. Zhang, Q. S. Jing, T. C. Hou, Z. L. Wang, *ACS Nano* **2012**, *6*, 10378.
[14] Z. L. Wang, *Adv. Mater.* **2012**, *24*, 4632.
[15] C. F. Pan, L. Dong, G. Zhu, S. M. Niu, R. M. Yu, Q. Yang, Y. Liu, Z. L. Wang, *Nat. Photon.* **2013**, *7*, 752.
[16] X. D. Wang, H. L. Zhang, R. M. Yu, L. Dong, D. F. Peng, A. H. Zhang, Y. Zhang, H. Liu, C. F. Pan, Z. L. Wang, *Adv. Mater.* **2015**, *27*, 2324.
[17] Q. Yang, X. Guo, W. H. Wang, Y. Zhang, S. Xu, D. H. Lien, Z. L. Wang, *ACS Nano* **2010**, *4*, 6285.
[18] Y. F. Hu, Y. Zhang, C. Xu, G. Zhu, Z. L. Wang, *Nano Lett.* **2010**, *10*, 5025.
[19] T. T. Pham, K. Y. Lee, J. H. Lee, K. H. Kim, K. S. Shin, M. K. Gupta, B. Kumara, S. W. Kim, *Energy Environ. Sci.* **2013**, *6*, 841.
[20] J. Shi, P. Zhao, X. D. Wang, *Adv. Mater.* **2013**, *25*, 916.
[21] Y. Zhang, G. Y. Gao, H. L. W. Chan, J. Y. Dai, Y. Wang, J. H. Hao, *Adv. Mater.* **2012**, *24*, 1729.
[22] L. Chen, M. C. Wong, G. X. Bai, W. J. Jie, J. H. Hao, *Nano Energy* **2015**, *14*, 372.
[23] B. P. Chandra, C. N. Xu, H. Yamada, X. G. Zheng, *J. Lumin.* **2010**, *130*, 442.
[24] A. N. Atari, *Phys. Lett.* **1982**, *90A*, 93.
[25] S. M. Jeong, S. Song, S. K. Lee, N. Y. Ha, *Adv. Mater.* **2013**, *25*, 6194.
[26] S. M. Jeong, S. Song, K. I. Joo, J. Kim, S. H. Hwang, J. Jeong, H. Kim, *Energy Environ. Sci.* **2014**, *7*, 3338.
[27] B. A. Evans, A. R. Shields, R. L. Carroll, S. Washburn, M. R. Falvo, R. Superfine, *Nano Lett.* **2007**, *7*, 1428.
[28] G. V. Stepanov, D. Y. Borin, Y. L. Raikher, P. V. Melenev, N. S. Perov, *J. Phys.: Condens. Matter* **2008**, *20*, 204121.
[29] J. Thevenot, H. Oliveira, O. Sandre, S. Lecommandoux, *Chem. Soc. Rev.* **2013**, *42*, 7099.
[30] B. A. Evans, B. L. Fiser, W. J. Prins, D. J. Rapp, A. R. Shields, D. R. Glass, R. Superfine, *J. Magn. Magn. Mater.* **2012**, *324*, 501.
[31] M. K. Tsang, G. X. Bai, J. H. Hao, *Chem. Soc. Rev.* **2015**, *44*, 1585.